

Supplementary Information for

5 Superstrong encapsulated monolayer graphene by the modified anodic bonding

Wonsuk Jung,^{‡^a} Taeshik Yoon,^{‡^a} Jongho Choi,^b Soohyun Kim,^a Yong Hyup Kim,^{*^b} Taek-Soo Kim,^{*}^a and Chang-Soo Han^{*^c}

^a Department of Mechanical Engineering, KAIST, Daejeon, 305-701, Republic of Korea,
¹⁰ tskim1@kaist.ac.kr

^b School of Mechanical and Aerospace Engineering, Seoul National University, Gwanak, Seoul 151-
744, Republic of Korea, yongkim@snu.ac.kr

^c School of Mechanical Engineering, Korea University, Anam, Seongbuk, Seoul 136-701, Republic of
Korea, cshan@korea.ac.kr

15 [‡] These authors contributed equally to this work.

* corresponding authors

Direct measurement of the adhesion energy of monolayer graphene using the DCB test.

DCB fracture mechanics tests were performed using a micromechanical tester, as shown in Fig.
20 S1. Specimens were inserted into the loading grips. The linear actuator with submicron resolution
controlled the displacement of the specimen. The load was measured simultaneously to obtain a load-
displacement curve.

We used heterogeneous beams; thus, the bending stiffness was different between the beams. To
ensure symmetric beam deformation during the DCB tests, the bending stiffness should be as similar
25 as possible. The dimensions and calculated bending stiffness values are provided in Table S1, where E'
is the plane strain modulus calculated from the Young's modulus and Poisson's ratio, I is the area

moment of inertia of the beam cross section, and $E'I$ is the bending stiffness. The glass was more compliant than the Si. Therefore, the glass thickness was greater than the Si thickness because bending stiffness is proportional to beam thickness by a power of three. Even the bending stiffness difference decreased to 34%; however, we modified the DCB test for more accurate calculations.

5

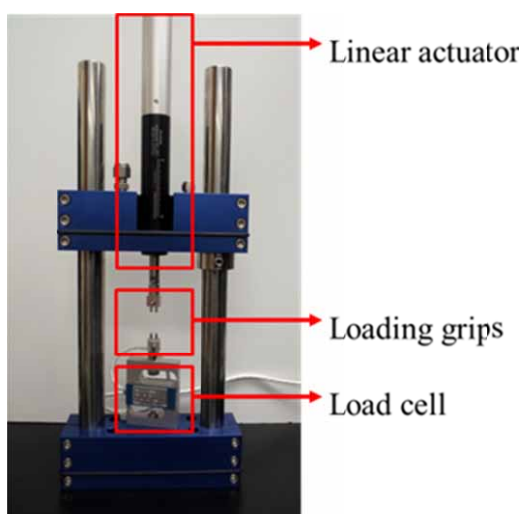


Figure S1. Double cantilever beam test equipment.

Table S1 Specimen dimensions and bending stiffness of silicon and glass beams

Material	Silicon	Glass
E' (Plane strain modulus)	170 GPa	65.6 GPa
B (Width)	5.75 mm	5.75 mm
h (Thickness)	550 μm	660 μm
I (Area moment of inertia)	$7.97 \times 10^{-14} \text{ m}^4$	$1.38 \times 10^{-13} \text{ m}^4$
$E'I$ (Bending stiffness)	$1.36 \times 10^{-2} \text{ Nm}^2$	$9.04 \times 10^{-3} \text{ Nm}^2$

10

From the load-displacement curve we can calculate the crack length at each loading/unloading cycle. Using basic solid and fracture mechanics, the crack length a , can be calculated by following equation,

$$a = \left(\frac{3C}{\frac{12}{E_1 B h_1^3} + \frac{12}{E_2 B h_2^3}} \right)^{1/3} \quad (1)$$

where, C is the specimen compliance which is obtained from the slope of load-displacement curve.

$$G_c = \frac{6P_c^2 a^2}{B^2} \left(\frac{1}{E_1 h_1^3} + \frac{1}{E_2 h_2^3} \right) \quad (2)$$

The adhesion energy G_c is defined as critical strain energy release rate, and it can be calculated by above equation. The P_c is critical load where the crack starts to propagate. The DCB test is composed of multiple loading/crack-growth/unloading cycles thus we can obtain multiple adhesion energy values from a specimen¹⁻³.

1. Kanninen. M.F. *et al.*, An augmented double-cantilever beam model for studying crack propagation and arrest. *International Journal of Fracture* **9**, 83-92 (1973).
10. Hohlfelder R.J. *et al.*, Adhesion of benzocyclobutene-passivated silicon in epoxy layered structures. *Journal of Materials Research* **16**(1), 243-255 (2001).
3. Yoon T. *et al.*, Direct measurement of adhesion energy of mono-layer graphene as grown on copper and its application to renewable transfer process. *Nano Lett.* **12**, 1448-1452 (2012).

15 Surface characterization of the fracture interface using optical microscopy

Optical images of the SiO₂ fracture interfaces displayed glass residue after separating the glass substrate from the SiO₂ in the DCB test. The glass residues shown in Fig. S2 illustrate that the amount of residue is dependent on the bonding energy. More glass residue remained on the substrate for interfaces with higher adhesion energies, as shown in Fig. S2.

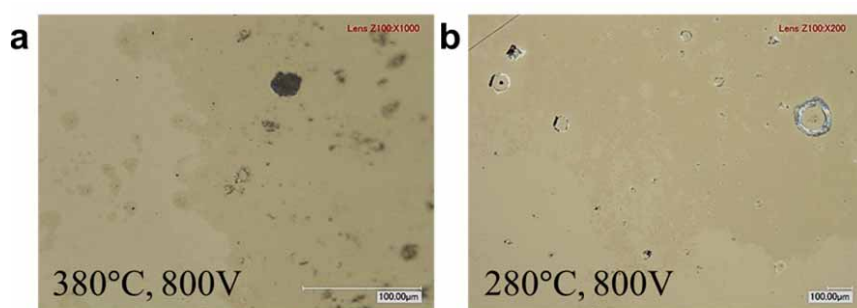


Figure S2. The optical images of fracture interface on the SiO₂ substrate after DCB Test.

Demonstration of adhesion energy of graphene adhesive

We demonstrated the actual application of suspending the heavy objects like Fig. 1d and S3. The tab for hanging the wire to maintain the object was attached to the bonded sample by epoxy, DP-420, 3M. This epoxy coated on the side of the tab to adhere the specimen. This tab was then fixed to the side of the glass substrate of the specimen after heating at 100°C for 15minutes. This specimen including the tab was similarly fixed to a large aluminum plate using epoxy.

Same tab was used to demonstrate another actual experiment of heavier object weighing 22kg like Fig. S3. After trying to suspend this object, the crack occurred in upper part of the glass substrate not the interface between graphene and glass or SiO₂ like Fig. S3. The left image of Fig. S3 shows the fracture interface of the glass substrate.

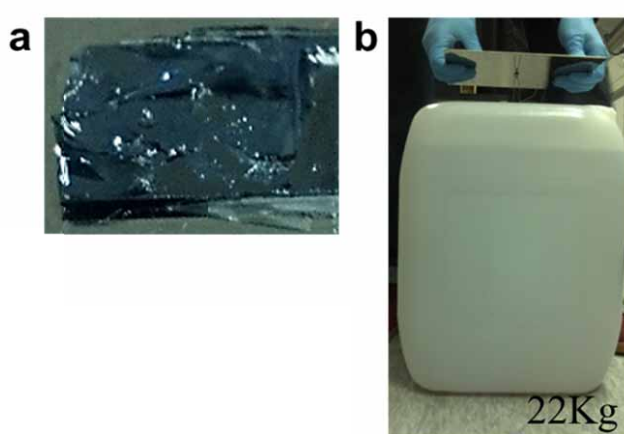


Figure S3. (a) Fracture interface in upper part of the glass not the bonded interface between graphene and each substrate. (b) Another heavier object weighing 22kg.

Control experiments without external voltage under identical conditions

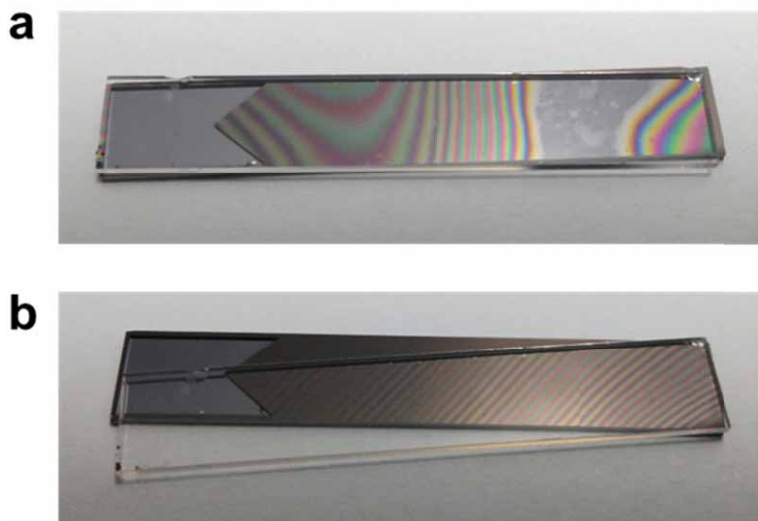


Figure S4. A control experiment without external voltage under identical temperature conditions.

Graphene was transferred to SiO_2 over the entire area of the substrate and then these samples were bonded to glass substrates. Newton's rings are observed over the entire area of graphene (a),(b), which means that this area is not bonded. (b) Moreover, these samples are easily detached from each other.